Supporting Information

Ching et al. 10.1073/pnas.1017069108

1. Model Equations

1.1. PY Cells. PYs are based on the model of McCarthy et al. (1). The membrane potential for each cell is given by:

$$\dot{v} = I_{\text{app}} - I_{\text{Na}} - I_{\text{K}} - I_{\text{Leak}}.$$

Sodium current:

$$I_{\text{Na}} = g_{\text{Na}}\, m^3 h (V - E_{\text{Na}}), \qquad \textbf{[S1]}$$

$$\dot{m} = \alpha_m(V)(1-m) - \beta_m(V)\, m$$

$$\dot{h} = \alpha_h(V)(1-h) - \beta_h(V)\, h$$

$$\alpha_m(V) = \frac{0.32(V+54)}{1-\exp(-(V+54)/4)}, \beta_m(V) = \frac{0.28(V+27)}{\exp((V+27)/5)-1}$$

$$\alpha_h(V) = 0.128(-(V+50)/18), \beta_h(V) = \frac{4}{1+\exp(-(V+27)/5)}$$

$$g_{\text{Na}} = 50, E_{\text{Na}} = 100$$

Potassium current:

$$I_{\text{K}} = g_{\text{k}}\, m^4 (V - E_{\text{K}}) \qquad \textbf{[S2]}$$

$$\dot{m} = \alpha_m(V)(1-m) - \beta_m(V)\, m$$

$$\alpha_m(V) = \frac{0.032(V+52)}{1-\exp(-(V+52)/5)}, \beta_m(V) = \frac{0.5(-(V+57)/40)}{40}$$

$$g_{\text{K}} = 80, E_{\text{K}} = -100$$

Leak current:

$$I_{\text{Leak}} = 0.1(V+61) \qquad \textbf{[S3]}$$

The applied current varies according to the number of cells and desired baseline spike rate. In the large simulation, the applied current is $I_{\text{app}} = 1.8 + I_{\text{u}}$, where $I_{\text{u}}\ N\ (0,0.1)$.

1.2. LTS Cells. LTS cells are based on the model of McCarthy et al. (1). The membrane potential for each cell is given by:

$$\dot{v} = I_{\text{app}} - I_{\text{Na}} - I_{\text{K}} - I_{\text{M}} - I_{\text{Leak}}.$$

The sodium, potassium, and leak currents are given in Eqs. S1–S3, respectively. M-current:

$$I_{\text{M}} = g_{\text{M}}\, m (V - E_{\text{M}})$$

$$\dot{m} = \alpha_m(V)(1-m) - \beta_m(V)\, m$$

$$\alpha_m(V) = \frac{0.0001 Q_s (V+30)}{1-\exp(-(V+30)/9)}, \beta_m(V) = \frac{-0.0001 Q_s (V+30)}{1-\exp((V+30)/9)}$$

$$g_{\text{M}} = 2, E_{\text{M}} = -100, Q_s = 3.209$$

In the large simulation, the mean applied current is $I_{\text{app}} = 1$.

1.3. FS Cells. FS cells are based on the model of Börgers et al. (2). The membrane potential for each cell is given by:

$$\dot{v} = I_{\text{app}} - I_{\text{Na}} - I_{\text{K}} - I_{\text{Leak}},$$

where the sodium, potassium, and leak currents are given by Eqs. S1–S3, respectively. In the large simulation, the mean applied current is $I_{\text{app}} = 0.55$.

1.4. TC Cells. TC cells are drawn from the work of Destexhe and colleagues (3–5). The membrane potential is given by:

$$\dot{v} = I_{\text{app}} - I_{\text{Na}} - I_{\text{K}} - I_{\text{T}} - I_{\text{h}} - I_{\text{Leak}},$$

Sodium current:

$$I_{\text{Na}} = g_{\text{Na}}\, m^3 h (V - E_{\text{Na}})$$

$$\dot{m} = \alpha_m(V)(1-m) - \beta_m(V)\, m$$

$$\dot{h} = \alpha_h(V)(1-h) - \beta_h(V)\, h$$

$$V_t = V + 35$$

$$\alpha_m(V) = \frac{0.32(13-V_t)}{\exp((13-V_t)/4)-1}, \beta_m(V) = \frac{0.28(V_t-40)}{\exp((V_t-40)/5)-1}$$

$$\alpha_h(V) = 0.128((17-V_t)/18), \beta_h(V) = \frac{4}{1+\exp((40-V_t)/5)}$$

$$g_{\text{Na}} = 90, E_{\text{Na}} = 50$$

Potassium current:

$$I_{\text{K}} = g_{\text{K}}\, m^4 (V - E_{\text{K}})$$

$$\dot{m} = \alpha_m(V)(1-m) - \beta_m(V)\, m$$

$$V_t = V + 25$$

$$\alpha_m(V) = \frac{0.032(15-V_t)}{\exp((15-V_t)/5)-1}, \beta_m(V) = \frac{0.5(10-V_t)}{\exp((10-V_t)/40)}$$

$$g_{\text{K}} = 10, E_{\text{K}} = -100$$

T-current:

$$I_{\text{T}} = g_{\text{Ca}}\, m_\infty^2 h (V - E_{\text{Ca}})$$

$$\dot{h} = (h_\infty - h)/\tau_h$$

$$V_t = V + 2$$

$$h_\infty = \frac{1}{(1+\exp((V_t+81)/4))}, m_\infty = \frac{1}{(1+\exp(-(V_t+57)/6.2))}$$

$$\tau_h = \frac{30.8+(211.4+\exp((V_t+113.2)/5))/(1+\exp((V_t+84)/3.2))}{3.73}$$

$$g_{\mathrm{Ca}} = 2, E_{\mathrm{Ca}} = 120$$

h-current:

$$I_{\mathrm{h}} = g_{\mathrm{h}}(o_1 + 2(1-c_1-o_1))(V-E_{\mathrm{h}})$$

$$\dot{o}_1 = 0.001(1-c_1-o_1) - 0.001((1-p_0)/0.01)$$

$$\dot{p}_0 = 0.0004(1-p_0) - 0.0004([\mathrm{Ca}]_i/0.002)^4$$

$$\dot{c}_1 = \beta(V)o_1 - \alpha(V)c_1$$

$$\beta(V) = (1-h_\infty)/\tau_s, \alpha(V) = h_\infty/\tau_s$$

$$h_\infty = 1/(1+\exp((V+75)/5.5))$$

$$\tau_s = 20 + 1000/((1+\exp((V+71.5)/14.2)) + (1+\exp(-(V+89)/11.6)))\mathrm{gh} = 0.25, E_{\mathrm{h}} = -40$$

[Ca]:

$$[\dot{\mathrm{Ca}}]_i = \frac{-10I_{\mathrm{T}}}{2\times 96489} + \frac{0.00024-[\mathrm{Ca}]_i}{5}$$

Leak current:

$$I_{\mathrm{Leak}} = 0.01(V+70) + 0.0172(V+100)$$

The TC cells do not receive background applied current.

1.5. RE Cells. The membrane potential is given by:

$$\dot{v} = I_{\mathrm{app}} - I_{\mathrm{Na}} - I_{\mathrm{K}} - I_{\mathrm{T}} - I_{\mathrm{Leak}},$$

Sodium current:

$$I_{\mathrm{Na}} = g_{\mathrm{Na}}\, m^3 h (V-E_{\mathrm{Na}})$$

$$\dot{m} = \alpha_m(V)(1-m) - \beta_m(V)\, m$$

$$\dot{h} = \alpha_h(V)(1-h) - \beta_h(V)\, h$$

$$V_t = V + 55$$

$$\alpha_m(V) = \frac{0.32(13-V_t)}{\exp((13-V_t)/4)-1}, \beta_m(V) = \frac{0.28(V_t-40)}{\exp((V_t-40)/5)-1}$$

$$\alpha_h(V) = 0.128((17-V_t)/18), \beta_h(V) = \frac{4}{1+\exp((40-V_t)/5)}$$

$$g_{\mathrm{Na}} = 200, E_{\mathrm{Na}} = 50$$

Potassium current:

$$I_{\mathrm{K}} = g_{\mathrm{K}}\, m^4 (V-E_{\mathrm{K}})$$

$$\dot{m} = \alpha_m(V)(1-m) - \beta_m(V)\, m$$

$$V_t = V + 55$$

$$\alpha_m(V) = \frac{0.032(15-V_t)}{\exp((15-V_t)/5)-1}, \beta_m(V) = \frac{0.5(10-V_t)}{\exp((10-V_t)/40)}$$

$$g_{\mathrm{K}} = 20, E_{\mathrm{K}} = -100$$

T-current:

$$I_{\mathrm{T}} = g_{\mathrm{Ca}}\, m^2 h (V-E_{\mathrm{Ca}})$$

$$\dot{h} = (h_\infty - h)/\tau_h$$

$$\dot{m} = (m_\infty - m)/\tau_m$$

$$V_t = V + 2$$

$$h_\infty = \frac{1}{(1+\exp((V+80)/5))}, m_\infty = \frac{1}{(1+\exp(-(V+52)/7.4))}$$

$$\tau_h = 22.7 + \frac{0.27}{(\exp((V+48)/4)+\exp(-(V+407)/50))}$$

$$\tau_m = 0.44 + \frac{0.15}{(\exp((V+27)/10)+\exp(-(V+102)/15))}$$

$$g_{\mathrm{Ca}} = 3, E_{\mathrm{Ca}} = 120$$

Leak current:

$$I_{\mathrm{Leak}} = 0.05(V+90)$$

The RE cells do not receive background applied current.

1.6. Synaptic Connectivity. Synaptic connectivity is modeled as follows:

AMPA:

$$I_{\mathrm{AMPA}} = g_{\mathrm{AMPA}}\, x (V-E_{\mathrm{AMPA}})$$

$$\dot{x} = 5(1+\tanh(V/4))(1-x) - x/2$$

where $E_{\mathrm{AMPA}} = 0$.

Similarly, for GABA:

$$I_{\mathrm{GABA}} = g_{\mathrm{GABA}}\, x (V-E_{\mathrm{GABA}})$$

$$\dot{x} = 2(1+\tanh(V/4))(1-x) - x/\tau_{GABA}$$

where $E_{\mathrm{GABA}} = -80$ and $\tau_{\mathrm{GABA}} = 5$.

The baseline conductances in the small models are as follows:

	PY	LTS	FS	RE	TC
g_{AMPA}	0.1	0.5	2	0.1	0.1
g_{GABA}	0.64	0.15	1	0.06	0.06

In the large model, all conductances are scaled according to the number of cells in the network.

Each cortical module has all-to-all connectivity between PY cells and INs and within the FS and LTS populations. No connectivity is established between the populations of FS and LTS cells or between individual PY cells. RE cells are all-to-all coupled with the PY cells, TC cells, and other RE cells. TC cells are are all-to-all coupled with PY, FS, and LTS, and RE cells. There is no connectivity between individual TC cells.

1.7. Noise. In the large model, in addition to a tonic drive, PY cells receive a Poisson noise train (i.e., for the j^{th} cell):

$$I_{\text{app},j}(t) = \bar{I}_{\text{app},j} + \bar{g}^s_{\text{E}} \exp(-(t - T(t))/\tau), \qquad \textbf{[S4]}$$

where $\bar{g}^s_E$ is a constant, τ is the decay time of excitation, and T (t) is a compound Poisson process of rate $1/f^j_s$.

$$T(t) = \min\{T_1, T_2, \ldots, T_{k-1}, T_k, \ldots | t < T(t)\} \qquad \textbf{[S5]}$$

where $T_k - T_{k-1}$ is an exponentially distributed random variable with mean $1/f^j_s$. Here, as in the work of Börgers et al. (2), $g^s_E = 0.02$ and $f^j_s = 10$.

2. Synchronization Index

The synchronization is based on the phase distribution between spiking events in two cells. Specifically,

$$SI = \frac{1}{N}\sqrt{\sum_{i=1}^{N} \sin^2\phi_i + \sum_{i=1}^{N} \cos^2\phi_i}$$

where ϕ_i is the phase difference between the i^{th} spiking events and *SI* is the Synchronization Index. This is a simple but informative metric for characterizing synchrony between spike trains. More details can be found in the article by Rosenblum et al. (6).

3. Analysis and Simulation Methods

The spectrogram in Fig. 1*A* was obtained using a 1-s window from a bipolar-referenced EEG signal. The global coherence in Fig. 1*C* was obtained by ordering the eigenvalues of the cross-spectral matrix associated with all channels in a nearest neighbor-referenced montage.

The spectrogram in Fig. 3*A* was obtained by simulating the network for 1 s for each level of propofol and computing the corresponding power spectrum based on the model EEG signal defined in Eq. **2**. The coherence in Fig. 3*B* was obtained from the two simulated EEG signals (from each cortical module) over the same 1-s windows.

The power spectrum in Fig. 6*A* was computed over a 10-s window using the membrane potential of TC cells. The spectra in Fig. 7*B* were computed over a 10-s window using the membrane potential of the cells in question.

A multitapered fast Fourier transform (with eight tapers), implemented in the Chronux data analysis package for MATLAB (Mathworks Inc.), was used for analysis (7).

4. Model Properties in Active Regimes

Consider again the small four-cell model but with no potentiation of $GABA_A$ and a higher level of background noise in the thalamic cells. Fig. S4 shows the network behavior when strong bursts of faster γ-range activity are evoked in both TC and PY cells. This simulation confirms that, in principle, with a more active parameterization, the thalamic cells can indeed serve their function as a relay of ascending excitation and a receiver of descending excitation. The particular frequencies involved would, naturally, depend on the specific activity being modeled as well as on the diversity of ionic currents and connectivity considered (features not included and future work are included in *Discussion*). Thus, the model presented here is not strictly limited to propofol conditions but could form a platform on which to examine broader regimes.

5. Additional Properties of LTS Cells and Network Behavior

The distinguishing feature of LTS cells in our model is the M-current, which gives the cortical part of the model the capability to produce a frequency increase in response to a low dose of propofol (i.e., the paradoxical excitation). This is demonstrated in Fig. S5*A*, where a PY-LTS pair is parameterized to fire at an α-baseline and a 100% GABA increase (i.e., a low dose) is applied at t = 5,000 ms. At t = 10,000 ms, GABA is increased to 200% and the frequency decreases to α. Other currents known to be present in LTS cells, such as I_h, were not included in the present model. When added, they do not significantly affect the network behavior. Fig. S5*B* shows the PY-LTS behavior when the h-current described by Jones et al. (8) is added to the LTS cell. Note that the frequencies at baseline change slightly, but the paradoxical excitation and high-dose α remain.

At higher propofol levels, the decay time of GABA is predominantly responsible for the cortical behavior, and the M-current plays a less significant role. To illustrate this, consider Fig. S6, which shows the four-cell model but with an FS cell in place of the LTS cell. At t = 5,000 ms, propofol is switched to a high-dose level and the thalamic cells become synchronized with cortical firing (compare with Fig. 4 in the text).

1. McCarthy MM, Brown EN, Kopell N (2008) Potential network mechanisms mediating electroencephalographic beta rhythm changes during propofol-induced paradoxical excitation. *J Neurosci* 28:13488–13504.
2. Börgers C, Epstein S, Kopell NJ (2005) Background gamma rhythmicity and attention in cortical local circuits: A computational study. *Proc Natl Acad Sci USA* 102:7002–7007.
3. Destexhe A, Bal T, McCormick DA, Sejnowski TJ (1996) Ionic mechanisms underlying synchronized oscillations and propagating waves in a model of ferret thalamic slices. *J Neurophysiol* 76:2049–2070.
4. Destexhe A, McCormick DA, Sejnowski TJ (1993) A model for 8-10 Hz spindling in interconnected thalamic relay and reticularis neurons. *Biophys J* 65:2473–2477.
5. Destexhe A, Sejnowski TJ (2001) *Thalamocortical Assemblies: How Ion Channels, Single Neurons and Large-Scale Networks Organize Sleep Oscillations.* (Oxford Univ Press, New York).
6. Rosenblum MG, Pikovsky A, Shafer C, Tass PA, Kurths J (2000) Phase synchronization: From theory to data analysis. *Neuro-informatics, Handbook of Biological Physics* (Elsevier Science, Amsterdam), Vol 4, pp 279–321.
7. Bokil H, Andrews P, Kulkarni JE, Mehta S, Mitra PP (2010) Chronux: A platform for analyzing neural signals. *J Neurosci Methods* 192(1):146–151.
8. Jones SR, Pinto DJ, Kaper TJ, Kopell N (2000) Alpha-frequency rhythms desynchronize over long cortical distances: A modeling study. *J Comput Neurosci* 9:271–291.

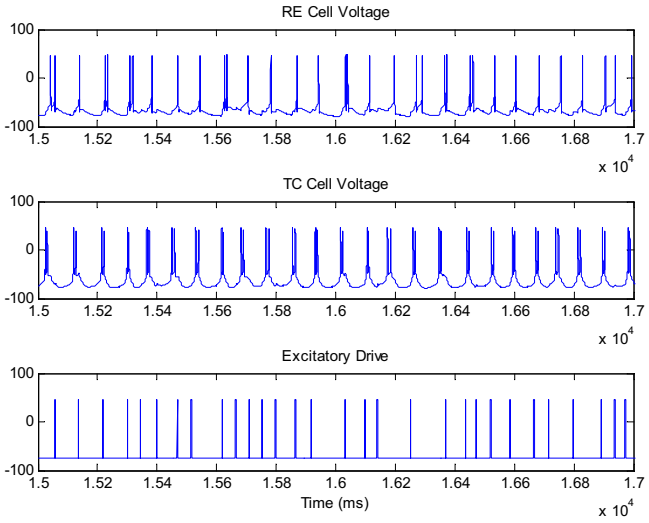

Fig. S1. Response of TC-RE cells under a high-propofol parameterization to random excitation. Despite the irregular input train, TC cells respond with persistent and periodical spiking (leading to the power spectral peak shown in Fig. 6*A*).

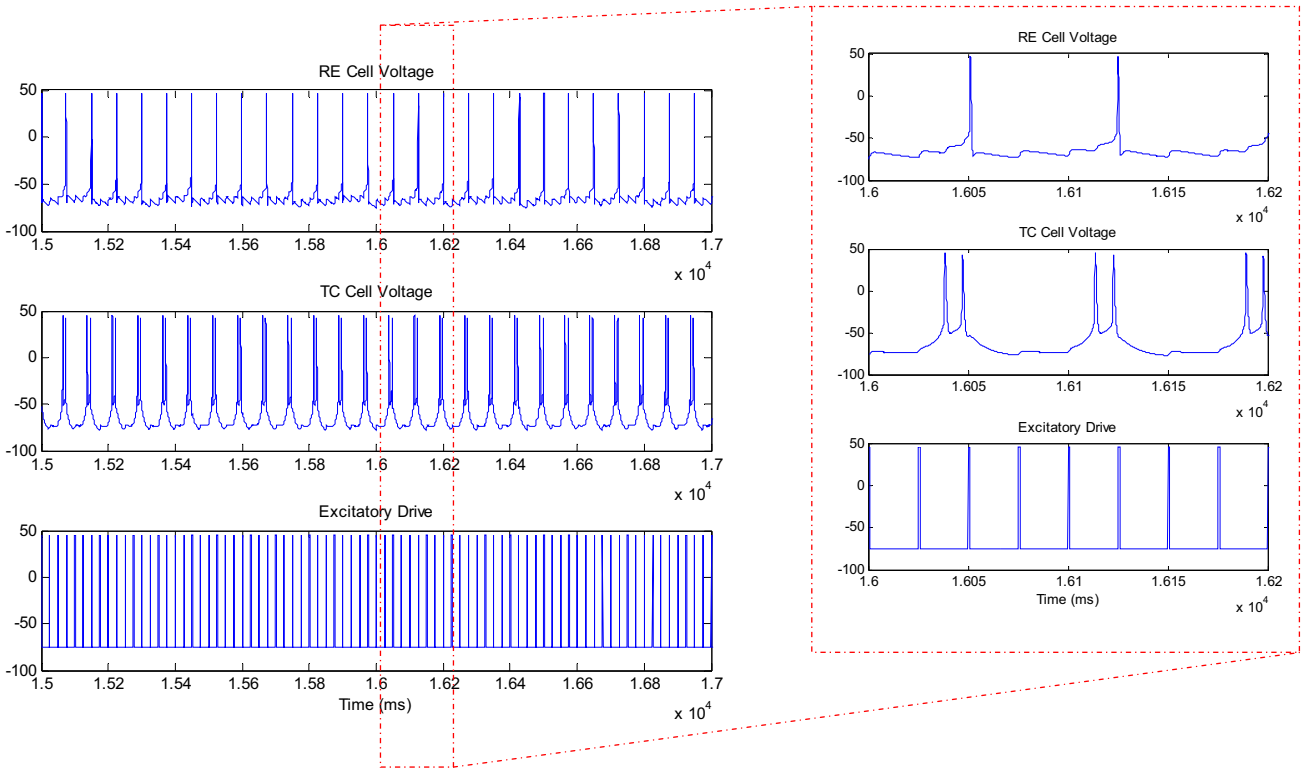

Fig. S2. Response of TC-RE cells under a high-propofol parameterization to 40-Hz periodic excitation. Although the input arrives at 40 Hz, the TC cells continue to produce α. The excitation is sufficient to sustain the natural frequency of the network; however, no additional spiking is evoked (additional details shown in Fig. S3).

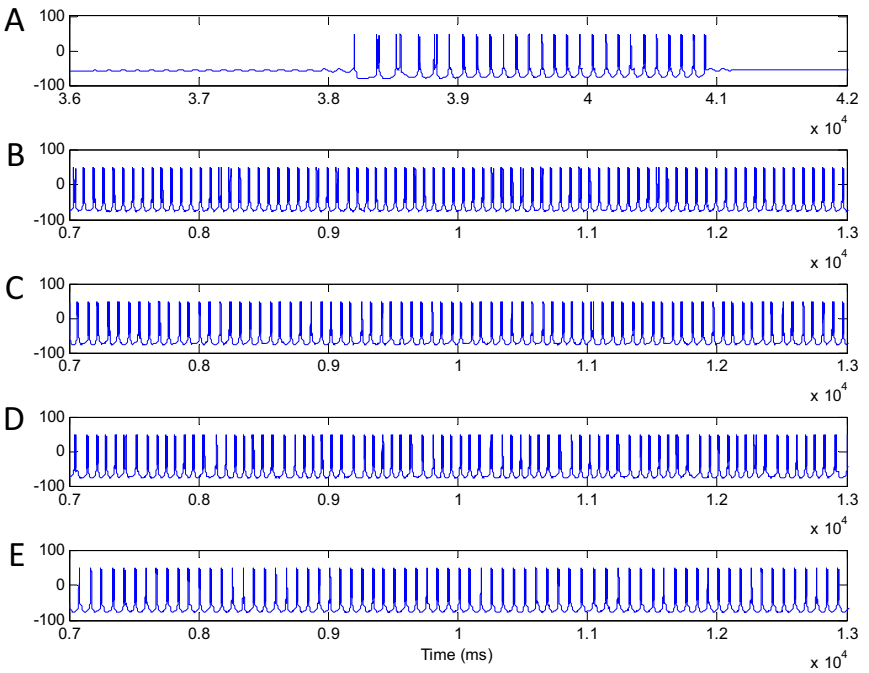

Fig. S3. Voltage traces of TC activity over 6 s under a high-propofol parameterization and no excitation (as in Fig. 6*C*) (*A*), 40-Hz excitation (as in Fig. S2) (*B*), 20-Hz excitation (*C*), 15-Hz excitation (*D*), and 6-Hz excitation (*E*). In all cases, the excitation is sufficient to yield uniform and sustained activity; however, the effect on the spiking frequency is minimal (it remains around 11 Hz). No additional spiking is evoked in the cases of 15, 20, and 40 Hz. Spiking does not slow in the 6-Hz case.

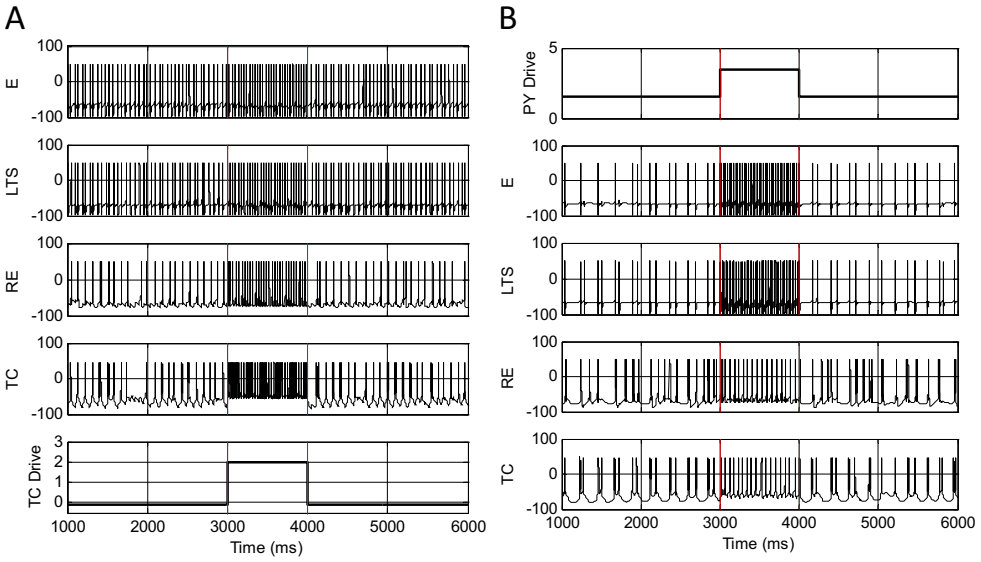

Fig. S4. Network properties are composite with active dynamic regimes. With no potentiation of GABA and increased thalamic background drive, a strong input to the thalamic cells evokes γ-activity that relays upward via the ascending thalamocortical connections (*A*) and a strong input to cortical cells evokes strong γ-activity that manifests in thalamic cells via the descending corticothalamic connections (*B*).

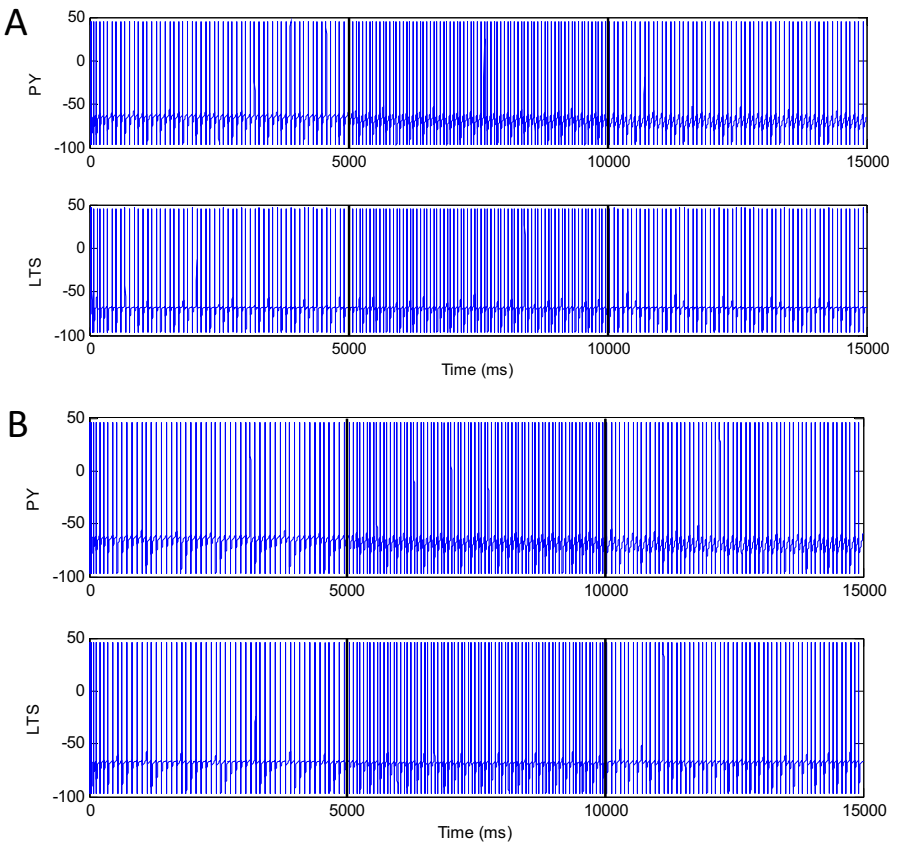

Fig. S5. (*A*) M-current allows for paradoxical increases in frequency in response to a low dose of propofol (t = 5,000 ms). A high dose enters at t = 10,000 ms. (*B*) Addition of *h*-current to LTS cells does not change the qualitative behavior in the cortical circuit.

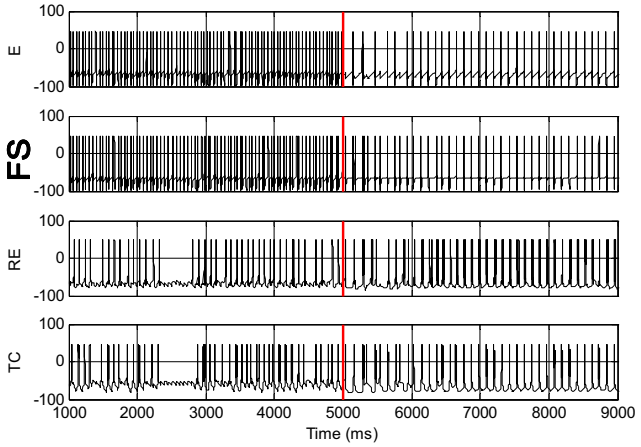

Fig. S6. Simulation of the four-cell model with an FS cell in place of an LTS cell. Propofol switches to a high dose at t = 5,000 ms.